BEND PROPAGATION IN FLAGELLA

I. Derivation of Equations of Motion and Their Simulation

Michael Hines and J. J. Blum, *Department of Physiology, Duke University Medical Center, Durham, North Carolina 27710 U.S.A.*

ABSTRACT A set of nonlinear differential equations describing flagellar motion in an external viscous medium is derived. Because of the local nature of these equations and the use of a Crank-Nicolson-type forward time step, which is stable for large Δt, numerical solution of these equations on a digital computer is relatively fast. Stable bend initiation and propagation, without internal viscous resistance, is demonstrated for a flagellum containing a linear elastic bending resistance and an elastic shear resistance that depends on sliding. The elastic shear resistance is derived from a plausible structural model of the radial link system. The active shear force for the dynein system is specified by a history-dependent functional of curvature characterized by the parameters m_0, a proportionality constant between the maximum active shear moment and curvature, and τ, a relaxation time which essentially determines the delay between curvature and active moment.

INTRODUCTION

Since bending waves pass along sperm tail flagella with little or no decrease in amplitude, energy must be generated locally. It is now well established that dynein arms, distributed on the A-subfibers of each outer doublet, form cross-bridges with the B-subfibers of adjacent doublets and thus provide the motive force for the filament sliding which underlies bend formation and propagation in cilia and flagella (Brokaw, 1975).

Machin (1958), in the first biophysical analysis of wave propagation in flagella, suggested that local active bending in one region of a flagellum would passively bend adjacent regions as a result of viscous resistance of the medium. If active bending were initiated locally by passive bending, a self-propagating wave would ensue. Brokaw (1966) modified Machin's model by assuming that active bending would be initiated after passive bending reached a critical value in the region immediately ahead of the actively bent section and derived an equation of motion for a flagellum consisting of two fibrils connected by shear-resistant elements. Lubliner and Blum (1971) extended this model by allowing a more realistic geometry of the fibrillar system. Use of a sliding filament model in these equations allowed a good fit to some data on the variation of wave speed with viscosity (Lubliner and Blum, 1972) and to the range of observed

initiation times (Lubliner and Blum, 1977). The equations developed by Lubliner and Blum, however, were limited to small-amplitude waves of nearly sinusoidal form.

Computer simulation of the large-amplitude equations was pioneered by Brokaw in a series of papers that examined successively more reasonable dynein cross-bridge systems (Brokaw, 1972*a*,*b*; Brokaw and Rintala, 1975, 1977). Brokaw's method is very general and easily allows simulation of arbitrary internal mechanisms. The method simulates the flagellum as a series of N straight-line segments of length Δs that bend only at the joints between segments. Motion of the flagellum in time is calculated by means of an explicit forward time step that involves inversion of a full $N \times N$ matrix at each time point. For reasonable values of N, the matrix inversions require a large amount of computing time and hence large time steps are needed to minimize computational cost. Unfortunately, if the only viscosity in the problem is the viscosity of the external medium, the explicit forward time step is computationally stable only for time steps satisfying the stability criterion $E_b \Delta t / C_N \Delta s^4 < \frac{1}{8}$, where E_b is the bending resistance coefficient and C_N is the normal viscous force coefficient (see Appendix A). Clearly for reasonable values of segment length, Δs, extremely small time steps are required to obtain a solution. For this reason, Brokaw (1972*a*) introduced an internal viscous bending resistance, C_b, and an internal viscous shear resistance, C_s. Use of these internal viscous resistances replaces the above stability criterion with a more lenient one and allows use of large time steps. Such a procedure is reasonable since the dynein system may display force-velocity behavior similar to that of muscle. An internal viscous resistance may mimic the essential aspects of such behavior.

With these viscous parameters, stable waves could be generated with a motile system in which the active bending moment generated by a sliding filament mechanism was locally controlled by curvature, κ, $\mathrm{d}M_a(s,t)/\mathrm{d}s = -m_0\kappa(s, t - \tau)$, where M_a is the active bending moment at any point, s is the distance along the flagellum and m_0 is a proportionality constant between active shear moment and curvature. The time delay, τ, is necessary to allow the active moment to also balance the moments due to the elastic bending resistance, E_b, and elastic shear resistance, E_s, that must be present in any model. Subsequently, Brokaw and Rintala (1975) showed that the introduction of a dynein system incorporating an active moment per unit length proportional to the mean shear displacement and dynein attachment functions proportional to curvature also yielded stable oscillating behavior (of course retaining the C_b and C_s parameters for stability).

Because of recent theoretical advances in setting up a realistic dynein system (e.g., Brokaw, 1976, and Brokaw and Rintala, 1977), there is no longer the need to model its viscous behavior with a separate viscous shear resistance. This brings to a head the stability problem and its deleterious effect on computational time and cost.

In what follows we develop an analysis based on local nonlinear differential equations that avoids the necessity of matrix inversions at each time step. This reduces the computing time by the order of the number of segments. More importantly, it makes possible a Crank-Nicolson type forward time integration step that is stable for rela-

tively large time steps, thus obviating the need for arbitrary internal viscous parameters.

Brokaw (1972*a*) found empirically that a cubic elastic shear resistance term was necessary to stabilize the bend amplitude. Lubliner (1973) showed on theoretical grounds that such behavior could be expected for small displacements of pinned radial links between the central and outer doublets. In view of the finding by Warner and Satir (1974) that the radial link system plays an important role in converting active sliding into bending, we have derived the behavior expected for a pinned radial link system during large sliding displacements, and thus introduce here a somewhat more realistic model for the radial link system than has hitherto been used. Use of this radial link model with a simple specification of the time dependence of shear force on curvature in conjunction with a highly efficient computer method for solving the nonlinear differential equations of motion have allowed us to generate stable propagating waves using only four parameters. A subsequent paper will deal with the flagellar motion when the shear force is generated by the attachment and detachment of dynein cross-bridges.

DERIVATION OF THE EQUATIONS OF MOTION OF A FLAGELLUM IN A VISCOUS MEDIUM

Description of Flagellar Shape

The flagellum is modeled as an inextensible thin filament of length L constrained to move in a plane (Fig. 1). The parameter s denotes distance along the flagellum ($0 < s < L$) and the vector $\mathbf{r}(s, t)$ describes the position of point s at time t. A particular resolution of $\mathbf{r}(s, t)$ with respect to a set of x and y coordinates fixed in the medium is

$$\mathbf{r}(s, t) = (x(s, t), y(s, t)). \tag{1}$$

Inextensibility of the flagellum imposes the constraint that $dx^2 + dy^2 = ds^2$. If we introduce the angle, $\alpha(s, t)$ between the flagellum and the x axis, then $dx = \cos \alpha ds$ and $dy = \sin \alpha ds$. Then

$$x(s, t) = x(0, t) + \int_0^s \cos(\alpha(s', t))\, ds', \tag{2a}$$

$$y(s, t) = y(0, t) + \int_0^s \sin(\alpha(s', t))\, ds' \tag{2b}$$

where $(x(0, t), y(0, t))$ is the motion of the proximal end of the flagellum. We now introduce a local coordinate system defined by the unit tangent and normal vectors at a point on the flagellum (see Fig. 1).

$$\hat{\mathbf{T}}(s, t) = \frac{\partial \mathbf{r}}{\partial s} = (\cos(\alpha(s, t)), \sin(\alpha(s, t))), \tag{3a}$$

$$\hat{\mathbf{N}}(s, t) = (-\sin \alpha(s, t), \cos(\alpha(s, t))) \tag{3b}$$

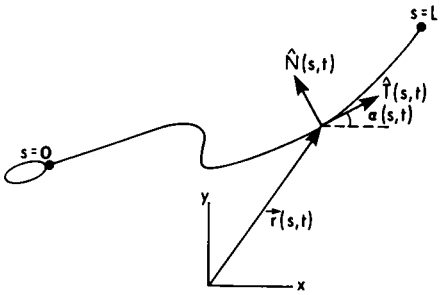

FIGURE 1

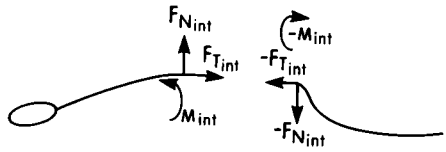

FIGURE 2

FIGURE 1 The vector $\mathbf{r}(s, t)$ describes the position of point s on the flagellum $(0 < s < L)$ at time t. Normal, $\hat{\mathbf{N}}$, and tangential, $\hat{\mathbf{T}}$, unit vectors are also shown. The variable $\alpha(s, t)$ measures the angle between $\hat{\mathbf{T}}$ and the x-axis.

FIGURE 2 The bending moments (M_{int}) and shear forces ($F_{N_{\text{int}}}$ and $F_{T_{\text{int}}}$) that must be applied to the cut ends of a flagellum to preserve its motion are shown.

Some relations that will be needed are:

$$\hat{\mathbf{T}} \cdot \hat{\mathbf{T}} = 1, \hat{\mathbf{N}} \cdot \hat{\mathbf{N}} = 1, \hat{\mathbf{T}} \cdot \hat{\mathbf{N}} = 0, \hat{\mathbf{T}} \times \hat{\mathbf{N}} = \hat{\mathbf{Z}}, \tag{4a}$$

where Z is a positive unit vector perpendicular to the plane, and

$$\partial \hat{\mathbf{T}}/\partial s = \hat{\mathbf{N}} \partial \alpha/\partial s, \qquad \partial \hat{\mathbf{T}}/\partial t = \hat{\mathbf{N}} \partial \alpha/\partial t \tag{4b}$$

$$\partial \hat{\mathbf{N}}/\partial s = -\hat{\mathbf{T}}(\partial \alpha/\partial s), \qquad \partial \hat{\mathbf{N}}/\partial t = -\hat{\mathbf{T}} \partial \alpha/\partial t. \tag{4c}$$

The normal and tangential velocity components at any point on the flagellum are then

$$\frac{\partial \mathbf{r}(s, t)}{\partial t} = V_N(s, t)\, \hat{\mathbf{N}}(s, t) + V_T(s, t)\, \hat{\mathbf{T}}(s, t). \tag{5}$$

Taking space derivatives of both sides of Eq. 5, one obtains

$$\frac{\partial^2 \mathbf{r}}{\partial s \partial t} = (\partial V_N/\partial s)\, \hat{\mathbf{N}} + V_N \partial \hat{\mathbf{N}}/\partial s + (\partial V_T/\partial s)\, \hat{\mathbf{T}} + V_T \partial \hat{\mathbf{T}}/\partial s, \tag{6}$$

which, upon substitution of the relations given in Eq. 4, becomes

$$\hat{\mathbf{N}} \partial \alpha/\partial t = (\partial V_N/\partial s + V_T \partial \alpha/\partial s)\hat{\mathbf{N}} + (\partial V_T/\partial s - V_N \partial \alpha/\partial s)\hat{\mathbf{T}}. \tag{7}$$

Equating the normal and tangential components on each side of Eq. 7 yields

$$\partial V_N/\partial s = \partial \alpha/\partial t - V_T \partial \alpha/\partial s, \tag{8}$$

$$\partial V_T/\partial s = V_N \partial \alpha/\partial s \tag{9}$$

Viscous Forces

We next use the Gray-Hancock approximation to relate the normal, $\phi_N(s,t)$, and tangential, $\phi_T(s,t)$, forces to the normal and tangential velocities, respectively, on an element ds.

$$\phi_N(s,t)\mathrm{d}s = -C_N V_N \mathrm{d}s \tag{10}$$

$$\phi_T(s,t)\mathrm{d}s = -C_T V_T \mathrm{d}s \tag{11}$$

The normal viscous drag coefficient, C_N, is taken in this paper to be twice that of the tangential drag coefficient, C_T, although a ratio of $C_N/C_T = 1.8$ may be more appropriate (Brokaw, 1970).

Bending Moment and Shear Force Equilibrium

If a flagellum were suddenly cut in two at some point s, two internal forces, $\mathbf{F}_{\text{int}}$, and a bending moment, M_{int}, would need to be applied at the cut end to retain the original motion of that point (Fig. 2).

To ensure that the flagellum does not accelerate, the total forces on the proximal end of the cut flagellum must sum to zero:

$$\mathbf{F}_E + \int_0^s \boldsymbol{\phi}(s',t)\,\mathrm{d}s' + \mathbf{F}_{\text{int}}(s,t) = 0, \tag{12}$$

where $\mathbf{F}_E$ represents any external force that may exist at $s = 0$.

Similarly, the total torque must equal zero to avoid angular acceleration:

$$T_E + \left\{ \int_0^s (\mathbf{r}(s',t) - \mathbf{r}(s,t)) \times \boldsymbol{\phi}(s',t)\,\mathrm{d}s' \right\} \cdot \mathbf{Z} + M_{\text{int}}(s,t) = 0 \tag{13}$$

where T_E is any external torque that may exist at $s = 0$. By differentiating Eqs. 12 and 13, it can be shown that

$$\partial \mathbf{F}_{\text{int}}(s,t)/\partial s = -\boldsymbol{\phi}(s,t) \tag{14}$$

$$\partial M_{\text{int}}(s,t)/\partial s = \{-\partial \mathbf{r}(s,t)/\partial s) \times \mathbf{F}_{\text{int}}(s,t)\} \cdot \hat{\mathbf{Z}}. \tag{15}$$

We now use the sign convention of Brokaw for consistency with his papers. He uses M and F to refer to external moments and shear forces. Thus $M = -M_{\text{int}}$ and $\mathbf{F} = -\mathbf{F}_{\text{int}}$. It is convenient to resolve $\mathbf{F}$ into its normal and tangential components as follows:

$$(\partial/\partial s)\mathbf{F} = \frac{\partial}{\partial s}(F_N \hat{\mathbf{N}} + F_T \hat{\mathbf{T}}) = \phi_N \hat{\mathbf{N}} + \phi_T \hat{\mathbf{T}}. \tag{16}$$

Upon substituting the relations given in Eq. (4), one obtains

$$\partial F_N/\partial s + F_T \partial \alpha/\partial s = \phi_N = -C_N V_N, \tag{17}$$

and

$$-F_N\partial\alpha/\partial s + \partial F_T/\partial s = \phi_T = -C_T V_T \tag{18}$$

Similarly,

$$\partial M/\partial s = (\partial \mathbf{r}/\partial s) \times (F_N\hat{\mathbf{N}} + F_T\hat{\mathbf{T}}) \cdot \hat{\mathbf{Z}}, \tag{19}$$

which, upon substitution of Eq. 3*a* and Eq. 4, becomes

$$\partial M/\partial s = F_N. \tag{20}$$

Eqs. 8, 9, 17, 18, and 20 comprise a set of differential equations that explicitly contain the external viscous forces and implicitly contain the geometrical constraints of flagellar motion. To proceed further it is necessary to specify the internal forces.

Internal Shear Forces and Bending Moments

Lubliner(1973) has shown that the moment generated by the internal mechanism of the flagellum is related to the flexural stiffness of the filaments and to effective shear force, S, by the following differential equation

$$\partial M_{\text{int}}/\partial s = -E_b\partial\kappa/\partial s - S, \tag{21}$$

where κ is the curvature, E_b the bending resistance, and S is the effective shear force due to sliding. Since $\kappa = \partial\alpha/\partial s$, $\partial M/\partial s = F_N$, and $M_{int} = -M$, Eq. 21 can be rewritten as

$$F_N = E_b\partial^2\alpha/\partial s^2 + S. \tag{22a}$$

S is given explicitly by

$$S = \sum\sum_{i>j} \frac{(y_i - y_j)}{\Delta s} S_{ij}, \tag{22b}$$

where y_i and y_j are the distance in the plane of bending of the ith and jth filaments from the neutral axis and S_{ij} is the tangential force component produced on the ith filament by a link or cross-bridge from the jth filament. The summation is taken over all filaments and for each filament over all connections within the length Δs, subject to the restriction that each link is only counted once.

In general, S_{ij} will be a function (or history-dependent functional) of the sliding $u_i - u_j$ between the ith and jth filaments. Since the filaments are not extensible, the change in amount of sliding per unit arc length is proportional to the change in bend angle, i.e.

$$\partial(u_i - u_j)/\partial s = (y_i - y_j)\partial\alpha/\partial s. \tag{23}$$

Hence

$$[u_i(s,t) - u_j(s,t)] - [u_i(0,t) - u_j(0,t)] = (y_i - y_j)[\alpha(s,t) - \alpha(0,t)]. \tag{24}$$

Note that the effective shear, γ, is defined as $\gamma(s,t) = (\mu_i(s,t) - u_j(s,t))/(y_i - y_j)$.

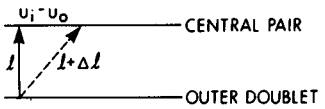

FIGURE 3

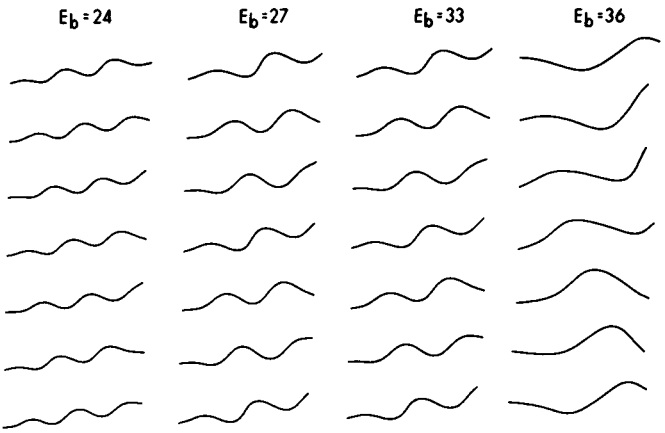

FIGURE 4

FIGURE 3 Geometry of stretching of a passive radial link due to filament sliding. The link is assumed to be pinned at both points of connection to the doublets, i.e. its resistance to sliding is due only to its resistance to stretch.

FIGURE 4 The effect of variation of E_b on flagellar shape. In each panel enough "snapshots" of the flagellum at 0.01 s intervals are presented to show at least one full beat cycle; shapes are successively displaced downward for clarity. E_b values for each simulation are shown (units: piconewtons times square micrometers). Values of other parameters were: $A_1 = 65$ pN; $m_0 = 130$ pN μm; $L = 30$ μm; $C_N = 0.005$ pN s/μm^2; $C_L/C_N = 0.5$; $\tau = 0.02$ s. Δs was 0.6 μm ($P = 50$), Δt was 0.001 s, and four iterations were used per time step. Computation time for one beat cycle took well under 5 s on an IBM 370 computer (IBM Corp., White Plains, N.Y.).

In this paper we will assume that there is a very high shear resistance near the origin of the flagellum, i.e. the filaments are tied together at the base. Generally, internal shear forces will arise from the radial link system and the dynein cross bridges. For a flagellum tied at the base, a large elastic shear force is also present at the base. [The passive links such as nexin (Stephens, 1974) may, for present purposes, be considered as part of the radial link system.] It is convenient to treat the dynein and the radial link systems separately, so that $S = S_d + S_r$.

Specification of Properties of the Radial Link System

Although the results of Warner and Satir (1974) indicate that the radial link system should be treated as a cross-bridge system, we here assume that the radial spoke system offers a passive elastic shear resistance to the sliding between the central pair and each outer doublet. Consider a spoke that is vertical and of length l when there is no shear, and is pinned at both ends so that it cannot develop any flexural force (Fig. 3).

The change in length after a sliding, $u_i - u_0$, between the ith outer doublet and the central pair is

$$l + \Delta l = l^2 + (u_i - u_0)^2. \tag{25}$$

If the Young's modulus of the spoke is E_s and its cross-sectional area is A, then the force developed along the spoke at the attachment sites is $EA\Delta l/l$, and the tangential component of force is then

$$S_{i0} = -\frac{EA\Delta l}{l}\frac{u_i - u_0}{l + \Delta l} = -\frac{EA(u_i - u_0)}{l}\left(1 - \frac{1}{\sqrt{1 + \left(\frac{u_i - u_0}{l}\right)^2}}\right). \tag{26}$$

If the average repeat distance for spokes is d_r then there are $\Delta s/d_r$ spokes attached to a single filament in distance Δs. Then from Eq. 22 we find the contribution of the radial link system to the shear force to be

$$S_r = -\frac{\Delta s}{d_r}\sum_{i=1}^{9}\frac{(y_i - y_0)}{\Delta s}\frac{EA(u_i - u_0)}{l}\left(1 - \frac{1}{\sqrt{1 + \left(\frac{u_i - u_0}{l}\right)^2}}\right) \tag{27}$$

Since the spokes are arranged in radial formation, $(y_i - y_0)/l = \sin(2\pi i/9 + \phi)$ where ϕ is some phase angle. Consequently,

$$S_r = -(EAl/d_r)\gamma\sum_{i=1}^{9}[\sin^2(2\pi i/9 + \phi)](1 - 1/\sqrt{1 + \gamma^2\sin^2(2\pi i/9 + \phi)}.) \tag{28}$$

When γ is small,

$$S_r \sim -(EAl/2d_r)\gamma^3\sum_{i=1}^{9}\sin^4(2\pi i/9 + \phi), \tag{29}$$

i.e. the cubic dependence of elastic shear used empirically by Brokaw (1972*a*). When γ becomes large,

$$S_r \sim -(EAl/d_r)\gamma\sum_{i=1}^{9}\sin^2(2\pi i/9 + \phi), \tag{30}$$

so that for large bend angles the elastic shear resistance changes from a dependence on γ^3 to a dependence on γ. For convenience in subsequent numerical analysis, the form

$$S_r = -A_1\gamma[1 - 1/\sqrt{1 + B_1\gamma^2}] \tag{31a}$$

was used, with A_1 and B_1 chosen so that for small and for large γ the value of S_r has the same value as in the complete sum of Eq. 28, i.e.

$$A_1 = (lEA/d_r)\sum_{i=1}^{9}\sin^2(2\pi i/9 + \phi) = 9lEA/2d_r, \tag{31b}$$

and

$$A_1B_1/2 = (lEA/2d_r)\sum_{i=1}^{9} \sin^4(2\pi i/9 + \phi)$$

$$= (3.38/2)EA/d_r; \text{ hence } B_1 = 0.75. \tag{31c}$$

Specification of the Active Shear Force

Before attempting to develop a statistical description of dynein cross-bridge kinetics, it was necessary to develop and test a computer program for simulation of the differential equations. For this purpose a simple two-parameter model for the hypothetical dependence of active shear force on curvature was chosen, i.e.

$$\tau \partial S_d/\partial t = -m_0 \partial\alpha/\partial s - S_d \tag{32}$$

Here $m_0\,\partial\alpha/\partial s$ is the maximum value of the active shear force that can be generated and the time constant, τ, is similar to Brokaw's (1972*a*) fixed time delay but has the advantage of being independent of the computational Δt.

Boundary Conditions and Initial Conditions

In this paper we are concerned with a flagellum with two free ends, where all forces and moments must vanish. Hence

$$F_N(0, t) = F_N(L, t) = 0, \tag{33a}$$

$$F_T(0, t) = F_T(L, t) = 0, \tag{33b}$$

$$M(0, t) = -E_b \left.\frac{\partial\alpha}{\partial s}\right|_{s=0} = 0; M(L, t) = -E_b \left.\frac{\partial\alpha}{\partial s}\right|_{s=L} = 0, \tag{33c}$$

$$\int_0^L S(s, t)\,ds = 0. \tag{33d}$$

Initial conditions are specified as an initial shape and initial shear force. If the initial conditions are specified so that they are inconsistent with the boundary conditions, then what happens physically is that the flagellum instantaneously adjusts its shape to comply with the boundary conditions.

Computer Solution of the Differential Equations of Motion

As noted above, Eqs. 8, 9, 17, 18, and 22*a* describe the motion of the flagellum in a viscous medium. A more useful description of the motion may be obtained by using Eqs. 8 and 9 to eliminate V_N and V_T from Eqs. 17 and 18. One then obtains

$$\partial^2 F_N/\partial s^2 = -C_N \partial\alpha/\partial t - (1 + C_N/C_T)(\partial F_T/\partial s)(\partial\alpha/\partial s) + (C_N/C_T)F_N(\partial\alpha/\partial s)^2 - F_T \partial^2\alpha/\partial s^2, \tag{34}$$

$$\partial^2 F_T/\partial s^2 = (1 + C_T/C_N)(\partial F_N/\partial s)(\partial \alpha/\partial s) + (C_T/C_N)F_T(\partial \alpha/\partial s)^2 + F_N \partial^2 \alpha/\partial s^2. \quad (35)$$

Eqs. 34 and 35, together with Eqs. 17, 18, and 22*a*, constitute a new set of nonlinear equations of motion for the flagellum. The computational advantage of this formulation can be most easily appreciated when F_N is a function (or history-dependent functional) of shape and contains no internal viscous terms, i.e. F_N and $\partial \alpha/\partial s$ are known at a particular instant and are independent of $\dot{\alpha}$. In this case, Eq. 35 is independent of $\dot{\alpha}$ and can be solved separately (and rapidly) to obtain F_T everywhere on the flagellum. Eq. 34 can then be solved for its only unknown, $\dot{\alpha}$. Knowledge of $\dot{\alpha}$ and the shape, α, at any moment permits one to find the shape at the next moment in time via an explicit forward time step, $\alpha(s, t + \Delta t) = \alpha(s, t) + \Delta t\, \dot{\alpha}(s, t)$, and then the new values of F_N and F_T, etc. Eqs. 17 and 18 can meanwhile be solved to obtain V_N and V_T for any point on the flagellum and numerically integrated in time to keep track of the translation of the flagellum through the medium.

It is well known that numerical solutions using such a forward time step (explicit method) are correct to order Δt. Appendix A, however, shows that the explicit method is unstable unless the size of the forward time step meets the rather severe stability criterion, $\Delta t < C_N(L/N)^4/8E_b$, where L is the length of the flagellum and N is the number of points used to approximate its shape. For a flagellum 40 μm long, approximated by 80 segments, with C_N and E_b values of 0.005 pN s/μm^2 and 30 pN μm^2, respectively, Δt must be less than $1.3 \cdot 10^{-6}$ s. To avoid the inordinate computational costs that the explicit method requires, we have applied the Crank-Nicolson procedure (see Smith, 1965), which is accurate to order $(\Delta t)^2$: $\alpha(s, t + \Delta t) = \alpha(s, t) + \Delta t\, \dot{\alpha}(s, t + 0.5\Delta t)$. As shown in Appendix A, the Crank-Nicolson method also has the advantage of being stable for large values of Δt, so that accurate solutions can be obtained with $\Delta t \sim 10^{-3}$ s. A full description of the computational procedure is given in Appendix B.

Choice of Parameter Values

According to Lubliner (1973), $E_b = E \sum_{i=1}^{10} I_i$, where E is Young's modulus (assumed equal for each filament) and I_i is the moment of inertia of each doublet. For the purposes of this computation, the central pair of singlet microtubules is considered equivalent to one outer doublet, so that the summation runs from 1 to 10. Following Lubliner and Blum (1971), we approximate the doublet shape as a rectangle of 0.037 μm $\times$ 0.024 μm. The moment of inertia for such a rectangularly shaped form is $I = ab(a^2 + b^2)/24$, where a and b are the dimensions of the sides of the rectangle. Hence $I = 7.2 \cdot 10^{-8}$ μm^4. Young's modulus for elastin is $\sim 0.06 \cdot 10^7$ pN/μm^2 and for collagen is about 10–100-fold larger (Milnor, 1974). Hence E_b is probably in the range of 0.4–40 pN/μm^2. Lubliner and Blum (1971) chose $E = 4$ dyn/μm^2, corresponding to $E_b \simeq 30$ pN μm^2.

To evaluate the elastic shear force, one needs to estimate the magnitude of A_1 in Eq. 31*b*. If a spoke is 4 nm in diameter and 60 nm long and if the average spacing be-

tween radial spokes is about 30 nm (Warner and Satir, 1974), then $A_1 = 9lEA/2d_r \sim 65$ pN, for a protein with a Young's modulus like elastin.

Brokaw (1972*a*) used a value of m_0 of ~130 pN μm; a comparable value can be computed from Eq. 22 is it is assumed that there are two dyneins per doublet spaced about 0.025 μm apart, that the dynein arms are about 60 nm long, that only four or five filaments are active at any one time, and that the maximal force exerted by a single dynein is about 4 pN (Brokaw, 1975).

Since τ is the primary determinant of frequency, a value of 0.02 s was chosen to give reasonable beat frequencies. C_N was taken as 0.005 pN s/μm^2, suitable for a flagellum in water.

RESULTS

Fig. 4 shows a sequence of print-outs of a flagellum 30 μm long swimming in a medium with the approximate viscosity of water for four different values of the bending resistance, E_b. These print-outs are taken after the transients have subsided. That stable wave forms have been achieved is evident. For E_b values between 27 and 33 pN μm^2 there was practically no change in wave shape, wave speed, beat frequency (~33 Hz) or swimming speed (~57 μm/s). There were almost two waves on the flagellum. When E_b was decreased to 24 pN μm^2, wave amplitude and wavelength decreased and the frequency increased to about 40 Hz, although τ remained constant at 0.02 s. Increasing E_b to 36 pN μm^2 increased the wavelength markedly, so that there was not even one full wave on the flagellum and frequency dropped to about 17 Hz. Whereas changes in E_b more than 20% above or below 30 pN μm^2 cause marked changes in wave parameters, increasing A_1 (see Eq. 31*a*) from 40 to 90 pN caused a smooth decrease in wave amplitude (simulations not shown). As m_0 increased from 100 to 150 pN μm, only slight changes in amplitude and wavelength were observed, but increasing m_0 to 160 pN μm decreased wavelength considerably so that another half wave was present. Decreasing m_0 to 90 pN μm caused an increase in wavelength such that flagellar shape resembled that obtained for $m_0 = 130$ pN by raising E_b to 36 pN μm^2.

τ is the dominant parameter in the control of beat frequency; as τ increased from 0.015 to 0.0275 s, frequency dropped from ~40 Hz to ~25 Hz with practically no change in wave shape. When $\tau = 0.03$ s, however, wavelength suddenly increased so that there was only one wave per flagellum and the frequency dropped to ~12 Hz.

Eqs. 22*a*, 32, 34, and 35 can be brought into a convenient nondimensional form by substituting $F_N^* = F_N L^2/E_b$, $t^* = E_b t/C_N L^4$, $s^* = s/L$, and $S_d^* = S_d L^2/E_b$. When this is done, Eq. 32 becomes

$$\frac{\tau E_b}{C_N L^4}\frac{\partial S_d^*}{\partial t^*} = -\frac{m_0 L}{E_b}\frac{\partial \alpha}{\partial s^*} - S_d^*. \tag{32a}$$

Since C_N enters into all the other equations as the ratio C_N/C_T or C_T/C_N, it can be seen that an increase in the viscous drag coefficient is equivalent to a decrease in τ (and a concomitant decrease in t*).

Increasing C_N from 0.005 to 0.03 pN s/μm^2 (maintaining $C_N = 2C_T$) caused a slight increase in amplitude and a decrease in frequency to about 20 Hz, with little change in shape. Above 0.03 pN s/μm^2 there was a sudden change in wavelength so that there were about three waves on the flagellum instead of two, and the frequency increased to about 25 Hz. Similar discontinuities in behavior in response to changes in viscosity were found in Brokaw's simulation studies (Brokaw, 1972*b*). These changes are not in accord with the observation that increasing viscosity in this range has a relatively small and smooth effect on both wavelength and frequency in sperm flagella. Brokaw (1972*b*) was able to simulate experimental observation by use of internal viscous resistance terms, so that external viscous forces had, necessarily, a limited effect. Introduction of a realistic dynein cross-bridge model instead of the purely formal mechanism used here (Eq. 32) is necessary to obtain results that agree with the observed effects of viscosity (and other factors such as temperature, ATP concentration, etc.) on wave shape and speed. Such studies are currently in progress.

We are grateful to Dr. J. Lubliner for helpful discussion.

This work was supported by National Science Foundation Grant BMS72-02520 A02.

Received for publication 25 November 1977 and in revised form 10 March 1978.

APPENDIX A

Stability Analysis

Consider a flagellum with only an elastic bending resistance, i.e. $S = 0$. Then, from Eq. 22 $F_N = E_b \partial^2\alpha/\partial s^2$. If the flagellum is nearly straight, all the second-order terms in Eq. 34 are small, and we have $\partial^2 F_N/\partial s^2 \simeq -C_N \partial\alpha/\partial t$. Eliminating F_N from these two equations yields

$$C_N \partial\alpha/\partial t + E_b \partial^4\alpha/\partial s^4 = 0. \tag{A1}$$

A finite difference approximation in the space domain using N points Δs apart yields a set of coupled ordinary differential equations

$$C_N \partial\alpha_p/\partial t + E_b(\alpha_{p-2} - 4\alpha_{p-1} + 6\alpha_p - 4\alpha_{p+1} + \alpha_{p+2})/\Delta s^4. \quad p = 1 \cdots\cdots N. \tag{A2}$$

The values for α_{-1}, α_0, α_{N+1}, and α_{N+2} are obtained from the boundary conditions (Eq. 33). N initial conditions are required to specify a unique solution to these N differential equations with N unknowns. If t is discretized as $t = q\Delta t$, the finite difference approximation to $\partial\alpha/\partial t$ in Eq. A1 is $\partial\alpha_p/\partial t\,|_{t=q\Delta t} = (\alpha_{p,q+1} - \alpha_{p,q})/\Delta t$ and Eq. A2 then becomes:

$$\alpha_{p,q+1} = \alpha_{p,q} - (r(\alpha_{p-2,q} - 4\alpha_{p-1,q} + 6\alpha_{p,q} - 4\alpha_{p+1,q} + \alpha_{p+2,q}), \tag{A3}$$

where $r = E_b \Delta t/C_N \Delta s^4$.

Since the value of α at the $q + 1$ time point is an explicit function of the value of α at the previous time point, this method of solution is called the explicit method; it converges to the correct partial differential equation to order Δt and $(\Delta s)^2$. Truncation errors are introduced at each step because computer operations are not completely accurate. If these errors do not grow, the method is said to be stable. Examination of the growth of errors during solution of

Eq. A3 may be done rigorously by matrix methods but a simple Fourier series method of Von Neumann (see Smith, 1965) will be used here. This analysis neglects the effects of boundary conditions on the solution, but they introduce no qualitative differences in the stability of Eq. A3. The errors, $E_{p,0}$, introduced at every point $p = 1 \cdots N$ at time $t = 0$ can be expressed as a finite Fourier series.

$$E_{p,0} = \sum_{n=1}^{N} A_n e^{i\pi np\Delta s/N\Delta s}.$$

Substituting this into Eq. A3 yields

$$E_{p,1} = \sum_{n=1}^{N} A_n [1 - r(e^{-2\pi in/N} - 4e^{-i\pi n/N} + 6 - 4e^{i\pi n/N} + e^{2\pi in/N})] e^{i\pi np/N},$$

$$= \sum_{n=1}^{N} A_n \xi_n e^{i\pi np/N}, \tag{A4}$$

Clearly,

$$E_{p,q} = \sum_{n=1}^{N} A_n \xi_n^q e^{i\pi np/N}. \tag{A5}$$

Eq. A5 shows that there will be no growth of error if $|\xi_n| < 1$ for all n. Since $\cos(2\pi n/N) = 2\cos^2(\pi n/N) - 1$, this criterion can be rewritten as $|\xi_n| = |1 - 4r[1 - \cos(\pi n/N)]^2| < 1$.

The term $[1 - \cos(\pi n/N)]^2 < 4$, and thus stability for the explicit method for a nearly straight flagellum requires that $r < \frac{1}{8}$, i.e.

$$\Delta t/\Delta s^4 < C_N/8E_b \tag{A6}$$

For the linear fourth-order equation (A2), one may improve on this stringent criterion for stability by use of the Crank-Nicolson implicit method. If one evaluates the equation at $t = (q + \frac{1}{2})\Delta t$ using $\alpha_p(t + \frac{1}{2}\Delta t) = \frac{1}{2}(\alpha_{p,q} + \alpha_{p,q+1})$, etc., then Eq. A3 becomes

$$r\alpha_{p-2,q+1} - 4r\alpha_{p-1,q+1} + (2 + 6r)\alpha_{p,q+1} - 4r\alpha_{p+1,q+1} + r\alpha_{p+2,q+1}$$
$$= -r\alpha_{p-2,q} + 4r\alpha_{p-1,q} + (2 - 6r)\alpha_{p,q} + 4r\alpha_{p+1,q} - r\alpha_{p+2,q}. \tag{A7}$$

This method converges to the correct solution of the partial differential equation to order $(\Delta t)^2$ and $(\Delta s)^2$. Stability can be analyzed as for the explicit method, and one obtains the criterion

$$|\xi_n| = \left| \frac{2 - 4r\left(1 - \cos\frac{n\pi}{N}\right)^2}{2 + 4r\left(1 - \cos\frac{n\pi}{N}\right)^2} \right| < 1. \tag{A8}$$

Since $|\xi_n| < 1$ for all r, there is no restriction on Δt for stability of the fourth-order linear differential equation (A1) when numerical solution is done by the Crank-Nicolson method. In practice, application of the Crank-Nicolson method to the nonlinear differential equations (34 and 35) is also stable.

APPENDIX B

Computational Procedure

To obtain the difference form of the differential equations the flagellum is approximated by $P + 1$ points, the first and last being the ends of the flagellum. Velocities, forces, and moments are then defined only at these points. Except at the boundaries, derivatives are replaced by their central differences, i.e.

$$\left.\frac{\partial \alpha}{\partial s}\right|_{i\Delta s} = \frac{\alpha_{i+1} - \alpha_{i-1}}{2\Delta s}, \quad \left.\frac{\partial^2 \alpha}{\partial s^2}\right|_{i\Delta s} = \frac{\alpha_{i+1} - 2\alpha_i + \alpha_{i-1}}{\Delta s^2},$$

with similar equations for the space derivatives of F_N and F_T. Substituting these central differences into Eq. 22a yields, for $i = 2 \cdots P$,

$$F_{N_i} = (E_b/\Delta s^2)(\alpha_{i+1} - 2\alpha_i + \alpha_{i-1}) + K_{S_i}(\alpha_i + \gamma_1 - \alpha_1) + S_{K_i}, \quad \text{(B1)}$$

where the total shear force, S, has been replaced by a term proportional to sliding, $K_{S_i}\gamma_i$, and all remaining terms not linearly proportional to sliding, S_{K_i}, for reasons to be clarified below. Note that from Eq. 24, $\gamma_i = \alpha_i + (\gamma_1 - \alpha_1)$. This allows one to use $\alpha_i (i = 2 \cdots P)$ and $(\gamma_1 - \alpha_1)$ as the independent variables determined by the equations of motion and the boundary conditions.

Similarly, Eqs. 34 and 35 become (for $i = 2 \cdots P$)

$$C_N \dot{\alpha}_i + \frac{1}{\Delta s^2}(F_{N_{i+1}} - 2F_{N_i} + F_{N_{i-1}}) - \{C_N(\alpha_{i+1} - \alpha_{i-1})^2/C_T 4\Delta s^2\} F_{N_i}$$
$$+ \left\{\frac{(1 + C_N/C_T)(F_{T_{i+1}} - F_{T_{i-1}})}{4\Delta s^2}\right\}(\alpha_{i+1} - \alpha_{i-1})$$
$$+ \{F_{T_i}/\Delta s^2\}(\alpha_{i+1} - 2\alpha_i + \alpha_{i-1}) = 0, \quad \text{(B2)}$$

and

$$F_{T_{i+1}} - 2F_{T_i} + F_{T_{i-1}} - \{C_T(\alpha_{i+1} - \alpha_{i-1})^2/4C_N\} F_{T_i}$$
$$= \tfrac{1}{4}(1 + C_T/C_N)(F_{N_{i+1}} - F_{N_{i-1}})(\alpha_{i+1} - \alpha_{i-1}) + F_{N_i}(\alpha_{i+1} - 2\alpha_i + \alpha_{i-1}), \quad \text{(B3)}$$

respectively.

The normal and tangential shear force boundary conditions, Eqs. 33*a* and 33*b*, become

$$F_{N_1} = F_{N_{P+1}} = 0 \text{ and } F_{T_1} = F_{T_{P+1}} = 0. \quad \text{(B4}a, \text{B4}b\text{)}$$

The moment boundary condition (Eq. 33*c*) (using a first-order forward difference for the proximal end and a first-order backward difference for the distal end) yields

$$\alpha_1 = \alpha_2 \text{ and } \alpha_{P+1} = \alpha_P. \quad \text{(B4}c\text{)}$$

Boundary condition (33*d*) becomes

$$\sum_{i=2}^{P} [K_{S_i}(\alpha_i + \gamma_1 - \alpha_1) + S_{K_i}] = 0 \quad \text{(B4}d\text{)}$$

The set of ordinary differential equations (B1–B3 and B4) is approximated by a set of algebraic equations by substituting a finite time difference equation for $\dot{\alpha}_i$, $\dot{\alpha}_i = [\alpha_i(t + \Delta t) - \alpha_i(t)]/\Delta t$ and evaluating all other variables at time $t + \theta\Delta t$ with a weighted average $\alpha(t + \theta\Delta t) = \theta\alpha_i(t + \Delta t) + (1 - \theta)\alpha_i(t)$. If $\theta = 0$ the algebraic equations are linear and can be solved explicitly for $\alpha(t + \Delta t)$. Such a procedure is correct to order Δt, but introduces serious stability problems (see Appendix A). If $\theta = 0.5$ (Crank-Nicolson method), the resulting algebraic equations are correct to order Δt^2 and stable, but are coupled and nonlinear. The choice $\theta = 1$ corresponds to a fully implicit method, which, like the Crank-Nicolson procedure, yields a coupled set of nonlinear algebraic equations but is correct only to order Δt. For the Crank-Nicolson and fully implicit methods, θ is greater than 0 and we can rewrite the weighted average as

$$\alpha_i(t + \Delta t) = (1/\theta)[\alpha_i(t + \theta\Delta t) - \alpha_i(t)] + \alpha_i(t). \tag{B5}$$

$\dot{\alpha}_i(t + \theta\Delta t)$ thus becomes $[\alpha_i(t + \theta\Delta t) - \alpha_i(t)]/\theta\Delta t$. F_{N_i} in the nonlinear algebraic equations corresponding to Eq. B2 can then be eliminated by using Eq. B1 and applicable boundary conditions. Collecting terms proportional to the various α_i yields (for $i = 2 \cdots P$)

$$\begin{aligned} R\alpha_{i-2}(t + \theta\Delta t) + \mathrm{LDIAG}_i\alpha_{i-1}(t + \theta\Delta t) + \mathrm{DIAG}_i\alpha_i(t + \theta\Delta t) \\ + \mathrm{UDIAG}_i\alpha_{i+1}(t + \theta\Delta t) + R\alpha_{i+2}(t + \theta\Delta t) \\ + \mathrm{COL1}_i(\gamma_1(t + \theta\Delta t) - \alpha_1(t + \theta\Delta t)) = \mathrm{RHS}_i(t), \end{aligned} \tag{B6}$$

where $R = E_b\Delta t/C_N\Delta s^4$; $\mathrm{LDIAG}_i = -4R - Rr_{2i} + r_1(K_{S_{i-1}} + F_{T_i} - r_{3i})$; $\mathrm{DIAG}_i = 6R + 2Rr_{2i} + r_1[-(2 + r_{2i})K_{S_i} - 2F_{T_i}] + 1/\theta$; $\mathrm{UDIAG}_i = -4R - Rr_{2i} + r_1(K_{S_{i+1}} + F_{T_i} + r_{3i})$; $\mathrm{COL1}_i = r_1[K_{S_{i-1}} - (2 + r_{2i})K_{S_i} + K_{S_{i+1}}]$; and $\mathrm{RHS}_i = -r_1[S_{K_{i-1}} - (2 + r_{2i})S_{K_i} + S_{K_{i+1}}] + \alpha_i(t)/\theta$. In these equations, $r_1 = \Delta t/C_N\Delta s^2$, $r_{2i} = (\alpha_{i+1} - \alpha_{i-1})^2C_N/4C_T$, $r_{3i} = (1 + C_N/C_T)(F_{T_{i+1}} - F_{T_{i-1}})/4$.

Eq. B6 with boundary condition B4*d* specifies a P by P matrix with column 1 ($i = 2 \cdots P$) given by $\mathrm{COL1}_i$, row 1 ($i = 2 \cdots P$) given by K_{S_i}, and $\mathrm{DIAG}_1 = \sum_{i=2}^{P} K_{S_i}$. The boundary conditions at the proximal end require that the second diagonal term is $\mathrm{DIAG}_2 + \mathrm{LDIAG}_2 + R$ and the third lower diagonal term is $\mathrm{LDIAG}_3 + R$, with $S_{K_1} = K_{S_1} = 0$. Similarly, the Pth diagonal term is $\mathrm{DIAG}_P + \mathrm{UDIAG}_P + R$ and the $P - 1$ upper diagonal term is $\mathrm{UDIAG}_{P-1} + R$, with $K_{S_{P+1}} = S_{K_{P+1}} = 0$. All other nonzero matrix coefficients are located on the two lower and two upper diagonals. $\mathrm{RHS}_1 = -\sum_{i=2}^{P} S_{K_i}$ completes the specification of the matrix equation. Note that the matrix coefficients of the $\alpha_i(t + \theta\Delta t)$ are themselves functions of α_i, F_{T_i}, S_{K_i}, and K_{S_i}. The matrix equations (including B4*d*) can be solved by the following iterative procedure, which converges to the correct solution of the set of nonlinear equations.

First, we compute the coefficients of the matrix at time t. The matrix equation is then rapidly solved by a Gauss elimination procedure, yielding a first approximation to $\alpha_i(t + \theta\Delta t)$ and $\gamma_1(t + \theta\Delta t) - \alpha_1(t + \theta\Delta t)$. These values are then used to solve for the F_{N_i} in Eq. B1, and this allows solution of Eq. B3 for F_{T_i}. These first approximations for $a_i(t + \theta\Delta t)$ and F_{T_i} are then used to obtain a new set of matrix coefficients, and these allow one to compute a second approximation to the $\alpha_i(t + \theta\Delta t)$ and $\gamma_1(t + \theta\Delta t) - \alpha_1(t + \theta\Delta t)$. The procedure can be repeated until all the α_i, F_{N_i}, and F_{T_i} are solutions to Eqs. B1 through B4 at time $t + \theta\Delta t$. We have found that four iterations are sufficient to satisfy the equations to the sixth decimal place. The solution can then be advanced to $\alpha_i(t + \Delta t)$ by use of Eq. B5.

Appendix A showed that the elastic bending resistance, E_b, appeared in the stability criterion for the explicit method. The presence of a restoring elastic shear force, $-E_S\gamma$, where

$E_S \equiv -S_r/\gamma$, introduces its own stability criterion of the form $\Delta t \sim C_N(\Delta s)^2/E_S$. For values of E_S in this paper, this stability criterion would require very small values of Δt for the iterative procedure to converge. To allow computation with large Δt, the two terms of the shear force, $S = S_d + S_r$, are treated separately.

S_d, the shear force arising from the dyneins, is, in this paper, computed at $t + 0.5\Delta t$ according to Eq. 32 from its known value at $t - 0.5\Delta t$ as follows:

$$(\tau/\Delta t)[S_d(t + 0.5\Delta t) - S_d(t - 0.5\Delta t)] = -(m_0/2\Delta s)(\alpha_{i+1}(t) - \alpha_{i-1}(t)) - \tfrac{1}{2}[S_d(t + \tfrac{1}{2}\Delta t) + S_d(t - \tfrac{1}{2}\Delta t)]. \quad \text{(B7)}$$

This, of course, is a straightforward computation, independent of the iterative procedure at $t + \theta\Delta t$. S_r, the shear force arising from the radial link system (including any contributions from nexin), will in general be a function of sliding, i.e. $S_r = f(\gamma)$. If we designate the amount of sliding occurring at the ith space point at the jth iteration step as γ_i^j, then S_r can be approximated by a Taylor expansion about γ_i^j as follows

$$S_r(\gamma_i^{j+1}) = S_r(\gamma_i^j) + \left.\frac{dS_r}{d\gamma}\right|_{\gamma_i^j}(\gamma_i^{j+1} - \gamma_i^j), \quad \text{(B8)}$$

where all of the γ_i terms are understood to be evaluated at $t + \theta\Delta t$. Hence $S_{K_i} = S_r(\gamma_i^j) - \gamma_i^j dS_r/d\gamma|_{\gamma_i^j} + S_{d_i}$, and $K_{S_i} = dS_r/d\gamma|_{\gamma_i^j}$. The filaments are tied together at the base by adding a very large linear elastic shear resistance term (-10^4 pN) to K_{S_2}. To minimize errors arising from incompatibility of the initial conditions with the boundary conditions, the solution at time $t = \Delta t$ (i.e. the first time step) is computed using the implicit method ($\theta = 1$). Since this is a single step in time, it is correct to order Δt^2. It should be stressed that any realistic form for dynein force generation can be handled according to this formalism.

Fig. 5 shows the effects of iteration number, size of time step, and the number of space points, P, on the computed shape of the flagellum after the transients have subsided. It can be seen that after two iterations there was no further apparent change in flagellar shape. Shape was independent of P for $P > 30$. The small differences that can be noted are due to the use of the first-order boundary conditions for the bending moments. Although the boundary conditions are first order for a homogeneous flagellum, they would become correct to second order if one assumed that the shear force vanished in the first and last segments. This means that the simulations shown for varying P are accurate but they represent slightly different physical situations, i.e. when $P = 30$, the shear force is defined to be zero within 1.5 μm of each end, while for

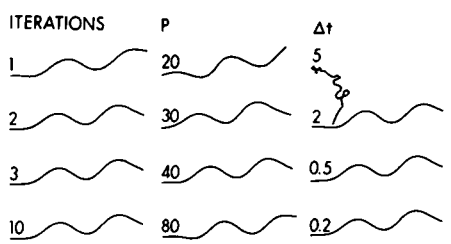

FIGURE 5 Effect of numerical parameters on the computation of steady wave shape. A 30-μm-long flagellum, initially arc-shaped, was allowed to evolve for 0.4 s with $E_b = 30$ pN μm^2, $A_1 = 65$ pN, $m_0 = 130$ pN μm, $C_N = 0.005$ pN s/μm^2. Unless otherwise labeled, $\Delta t = 1$ ms, $P = 40$ ($\Delta s = 0.75$ μm) and the number of iterations was four.

$P = 80$, it is zero within 0.375 μm of each end. For a Δt of 0.005 s a stable solution was not obtained. For Δt of 0.002 s or less, however, there was no difference in shape. Clearly, simulations with $\Delta t = 0.001$ s, $P = 50$, and four iterations, as in Fig. 4, are reliable.

REFERENCES

BROKAW, C. J. 1966. Bend propagation along flagella. *Nature (Lond.).* **209**:161.

BROKAW, C. J. 1970. Bending moments in free-swimming flagella. *J. Exp. Biol.* **53**:445.

BROKAW, C. J. 1972*a*. Computer simulation of flagellar movement. I. Demonstration of stable bend propagation and bend initiation by the sliding filament model. *Biophys. J.* **12**:564.

BROKAW, C. J. 1972*b*. Computer simulation of flagellar movement. II. Influence of external viscosity on movement of the sliding filament model. *J. Mechanochem. Cell Motility* **1**:203.

BROKAW, C. J. 1975. Cross bridge behavior in a sliding filament model for flagella. *In* Molecules and Cell Movement. S. Inoue and R. E. Stephens, editors. Raven Press, New York. 165–179.

BROKAW, C. J. 1976. Computer simulation of flagellar movement. IV. Properties of an oscillatory two-state cross bridge model. *Biophys. J.* **16**:1029.

BROKAW, C. J., and D. RINTALA. 1975. Computer stimulation of flagellar movement. III. Models incorporating cross-bridge kinetics. *J. Mechanochem. Cell Motility.* **3**:77.

BROKAW, C. J., and D. RINTALA. 1977. Computer simulation of flagellar movement. V. Oscillation of cross-bridge models with an ATP-concentration-dependent rate function. *J. Mechanochem. Cell Motility.* **4**:205.

LUBLINER, J. 1973. An analysis of interfilament shear in flagella. *J. Theor. Biol.* **41**:119.

LUBLINER, J., and J. J. BLUM. 1971. Model for bend propagation in flagella. *J. Theor. Biol.* **31**:1.

LUBLINER, J., and J. J. BLUM. 1972. Analysis of form and speed of flagellar waves according to a sliding filament model. *J. Mechanochem. Cell Motility* **1**:157.

LUBLINER, J., and J. J. BLUM. 1977. Analysis of bend initiation in cilia according to a sliding filament model. *J. Theor. Biol.* In press.

MACHIN, K. E. 1958. Wave propagation along flagella. *J. Exp. Biol.* **35**:796.

MILNOR, R. W. 1974. Principles of hemodynamics. *In* Medical Physiology, Vol. 2. V. B. Mountcastle, editor, The C. V. Mosby Co., St. Louis, Mo. 921.

SMITH, G. D. 1965. Numerical Solution of Partial Differential Equations. The Oxford University Press, London.

STEPHENS, R. E. 1974. Enzymatic and structural proteins of the axoneme. *In* Cilia and Flagella. M. A. Sleigh, editor. Academic Press, Inc., New York. 39–76.

WARNER, F. D., and P. SATIR. 1974. The structural basis of ciliary bend formation. Radial spoke positional changes accompanying microtubule sliding. *J. Cell Biol.* **63**:35.